Preparation of $LiFePO_4$-Based Electrodes with Magneto-Sensitive Iron Oxide (Fe_2O_3) Nanoparticles Under Magnetic Field

Emmanuel Iheonu Nduka (Master's Student)

Submitted in fulfillment of the requirements for the Master of Science degree in Chemical and Materials Engineering

School of Engineering and Digital Science

Department of Chemical and Materials Engineering, Nazarbayev University

53 Kabanbay Batyr Avenue, Astana, Kazakhstan, 01000

Lead Supervisor: Zhumabay Bakenov

Co-supervisor: Dr. Aliya Mukanova

Date: April 7, 2024

Declaration

I, at this moment, declare that this manuscript, entitled "Preparation of $LiFePO_4$-Based Electrodes with Magneto-Sensitive Iron Oxide (Fe_2O_3) Nanoparticles Under Magnetic Field," is the result of my work except for quotations and citations, which have been duly acknowledged.

I also declare that, to the best of my knowledge and belief, it has not been previously or concurrently submitted, in whole or in part, for any other degree or diploma at Nazarbayev University or any other national or international institution.

Emmanuel Iheonu Nduka

Date: 15th March 2024

Abstract

Lithium iron phosphate ($LiFePO_4$) is one of the most widely utilized cathode materials in lithium-ion batteries (LIBs) due to its low cost and environmental safety. Despite this attribute, they still face significant challenges, including high rates and prolonged cycling. However, research has shown that utilizing a magnetic field (MF) can help tackle these issues, thereby improving the ion conductivity and inhibiting polarization of the $LiFePO_4$ cathode. In this study, $LiFePO_4$ cathodes were produced by subjecting them to MF (LFP-MF), while others were optimized using magnetic-sensitive Fe_2O_3 nanoparticle additives in two concentrations (LFP+1 wt% Fe_2O_3-MF and LFP+3 wt% Fe_2O_3-MF). The cathodes were compared to conventional $LiFePO_4$ electrodes prepared under the same conditions but without applying MF (LFP-WMF, LFP+1% Fe_2O_3-WMF, and LFP+3% Fe_2O_3-WMF). Application of MF improved the materials' electrochemical properties, contributing to the battery's superior electrochemical performance. The lithium-ion diffusion coefficients of LFP-MF (4.1376×10^{-4} cm^2 S^{-1}), LFP+1% Fe_2O_3-MF (4.0614×10^{-4} cm^2 S^{-1}), and LFP+3% Fe_2O_3-MF (2.3021×10^{-4} cm^2 S^{-1}) were more significant than those of $LiFePO_4$ cathodes without subjecting to the magnetic field. Furthermore, the cathodes subjected to MF had higher reversible capacity and a reduced capacity decay than those without MF at an enhanced rate capability greater than 1 C. This study discovered that an MF improves the high-rate performance of $LiFePO_4$ cathodes.

KEYWORDS: lithium-ion battery, lithium iron phosphate, iron (III) oxide (Fe_2O_3), magnetic field, rate capacity, diffusion coefficient

Acknowledgment

Firstly, my sincere appreciation goes to my lead supervisor, Professor Zhumabay Bakenov, my co-supervisor, Dr. Aliya Mukanova, and my group colleague, Mrs. Nazgul Assan, for their support in all aspects of this work, including daily and weekly meetings, mentorship, advice, and for providing me with all the necessary materials and guidelines that have helped during this project. Despite their daily schedules, they have always made themselves available to instruct me on things to do and have always given positive recommendations and guidance that have led to the achievement of the work.

Further, I want to use this opportunity to appreciate my coursemates Mutiat Oniye and Andy Kofi, my colleagues, especially Mr. Emmanuel Chisom Nwaogu, Mr. Nurbolat Issatayev, Mr. Mukagali Yegamkulov, Ms. Guldana Alimbetova, Mr. Mukushev IIyas and the entire advanced materials energy and application lab (Battery Group) for their support so far in exchanging knowledge with me which has also supported my progress so far; you guys were amazing.

My heartfelt appreciation goes to Nazarbayev University and its management for allowing me to study in an exceptional environment equipped with quality research laboratories and multicultural exposure and to grow an excellent network with prominent scholars of diverse backgrounds. This accomplishment has been a turning point in my scholarly pursuit, exposing me to receiving a well-rounded education.

Finally, my sincere gratitude goes to my lovely parents, Engr. Emmanuel Amaobi Iheonu and my brothers and sisters for their unwavering love, care, emotional and mental support, prayers, and core values. I will forever be indebted to you for all your support. I also want to thank everyone who assisted me in one way or another during this process. Thank you all.

Table of Contents

List of Abbreviations and Symbols

Fe_2O_3	Iron (III) Oxide
MNPs	Magnetic Sensitive Nanoparticles
MF	Magnetic Field
XRD	X-ray Diffraction
SEM	Scanning Electron Microscope
CV	Cyclic Voltammetry
PVDF	Polyvinylidene Fluoride
AB	Acetylene Black
$LiPF_6$	Lithium hexafluorophosphate
EC	Ethylene carbonate
DMC	Dimethyl carbonate
EIS	Electrochemical AC Impedance Spectroscopy
LIB	Lithium-ion Battery
$LiFePO_4$/LFP	Lithium iron phosphate
NMP	N-Methyl-2-Pyrrolidone
WMF	Without Magnetic Field
Li^+	Lithium-ion
Li-S	Lithium-sulfur Batteries
$Li\text{-}O_2$	Lithium-oxygen Batteries

MHD	Magnetohydrodynamic
NMR	Nuclear magnetic resonance
EMR	Electromagnetic spectrum
$LiMn_2O_4$	Lithium manganese spinel

List of Figures and Tables

List of tables

1.0. Chapter One – Introduction

Globally, lithium-ion batteries (LIBs) are an essential energy storage system for daily human existence, with their main applications exceeding portable electronics and vehicles, but also provide distinct benefits for power storage. They emerged as the most popular lithium-based battery system due to their high energy density, high voltage performance, low self-discharge, lack of memory effect, superior cycle performance, and strong rate performance [1-3]. Their fundamental components include the anode, cathode, electrolyte, and separator, which also determine the electrochemical performance of LIBs [2]. Among these components, the cathode and anode materials are expected to have excellent electronic and ionic conductivity, allowing for reversible lithium-ion (Li^+) insertion and extraction [2]. Thus, to achieve this, they must have a suitable lattice structure, crystallinity, and structural stability to fulfill the requirements of the rocking chair battery model [2, 4].

In LIBs, lithium iron phosphate ($LiFePO_4$) is regarded as one of the most used cathode materials due to its outstanding electrochemical performance, safety, ecologically favorable features, and inexpensive raw material costs [5, 6]. However, its downside includes relatively low average potential, poor rate capacity, weak electron conductivity, low Li^+ diffusion coefficient, and low volumetric specific capacities across electrodes. This results in capacity decay at high charge-discharge density, reducing the applicability of the $LiFePO_4$ cathode material [2, 5, 6]. Notwithstanding, research has shown that utilizing a magnetic field (MF) can improve the ion conductivity of $LiFePO_4$ cathode electrode materials, promoting high rate and cyclic performance [2, 5, 6, 7, 8]. Studies have demonstrated that when an MF is applied in the synthetic process of electrode materials, the nucleation and growth processes shift, resulting in anisotropy and modifying the crystal lattice. This process is due to decreased surface energy, directional expansion along the easy axis, and increased dipoles [2, 9]. Further, it was shown that when magnetic moments of material are exposed to an MF, they exhibit a precise level of magnetism known as magnetization [2]. This approach modifies the crystal orientation, resulting in an orientated crystal structure that promotes lithium storage and diffusion [10]. Moreover, when an MF is imposed perpendicular to a $LiFePO_4$ electrode surface, the tiny crystals align along the b-axis (010) coordinate, parallel to the half-cell's operating direction [5, 11]. This

process increases Li^+ diffusion along the channel. Thus, an MF can induce channel direction, facilitating Li^+ transport, thereby increasing high-rate, cyclic performance and reducing concentration polarization in LIBs [2, 6, 11].

Recently, the use of magnetic sensitive nanoparticles (MNP) to enhance the electrochemical performance of LIB cathode has gained attention. It has been investigated that when MNPs are introduced to cathode material, they improve electrochemical and structural properties due to the presence of metal oxide. However, in the synthesis of $LiFePO_4$, Fe_2O_3 has been seen as a promising MNP due to its abundance, chemical stability, high theoretical specific capacities, low cost, and environmentally friendly attributes [12, 13]. According to [14], Fe_2O_3 nanoparticles with electrically conductive coating layers enhance the battery's electrochemical capabilities by improving electrical conductivity, redox reversibility, and shorter lithium ion and electron transit lengths. Consequently, researchers have suggested that incorporating Fe_2O_3 into the electrode offers a simple and less expensive strategy to enhance the power density and cycle life of LIBs [12, 15].

Many efforts to improve electrochemical performance have focused on internal strategies, such as modifying or upgrading cell components by coating, particle size reduction, and so on. These internal approaches can improve electrochemical performance, but they have drawbacks. For example, changes in the cell environment, such as additives and electrode modifications, create concerns about cell stability [16]. However, using an external method such as an MF to increase electronic conductivity and improve the electrochemical properties of the LIBs cathode has been identified as a particularly effective technique. This method can be used efficiently to enhance particle alignment, reduce particle agglomeration, improve electrode porosity, promote lithium-ion diffusion, and reduce internal resistance on the cathode [5, 17]. Hence, in this study, we evaluate the influence of an MF and MNP (Fe_2O_3) on fast-charging LIBs utilizing a permanent magnet with an intensity of 0.3 T during cathode (slurry) fabrication to optimize the structural and electrochemical performance of $LiFePO_4$. In contrast to the results reported in [6] and [5], we employed a commercial active material ($LiFePO_4$) while mixing it with Fe_2O_3 MNPs during slurry synthesis and placed it under a permanent magnet intensity of 0.3 T. As a result, decreasing the MF from 6 and 0.5 to 0.3 T makes it easy to incorporate the MF process into LIB plants' large production lines. However, the findings of this study show that, unlike $LiFePO_4$

cathodes without MF placement, MF-dried cathodes have better electrochemical performance, less polarization, increased Li^+ diffusion, and improved capacity retention. This is a significant advance compared to the reported work [6], where the authors used a 6 T superconducting magnet cooled with liquid helium, which is expensive and cannot be used in real battery plant production.

1.1. Aim of the project

This project aims to develop a reliable MF method for producing high-performance LIBs with stable cyclability and fast charging. To accomplish this, the performance of the lithium-ion cathode material was enhanced during cathode fabrication by applying a permanent magnet with an intensity of 0.3 T. Also, the slurries were further examined for the effect of MF (0.3 T) placement combined with magneto-responsive composite-iron (III) oxide additive to $LiFePO_4$ during cathode preparation.

1.2. Hypothesis and goals

The hypothesis of this work focuses on applying an external MF combined with iron (III) oxide (Fe_2O_3) during cathode slurry preparation. The MF is expected to enhance the ion alignment, uniform deposition of $LiFePO_4$ in the cathode, and reduce polarization, while the Fe_2O_3 helps enhance the active material's magnetic properties ($LiFePO_4$). Thus, this process contributes to a better electrochemical performance of the battery and improves electrochemical characteristics in the material, resulting in faster charging, higher rate performance, and better cyclic stability.

2.0. Chapter Two – Literature Review

2.1. History of Lithium Batteries

Lithium was found through analysis of petalite ore by Arfwedson and Berzelius in 1817 [18]. In 1821, William Thomas Brande and Sir Humphry Davy isolated lithium by electrolyzing lithium oxide. This process indicated the actual extraction of the element lithium. Despite its discovery and extraction in antiquity, scientists such as Gilbert N. Lewis had to wait almost a century to start studying the electrochemical characteristics of lithium due to delays in the development of lithium's prospective applications [18]. However, lithium is a good material for batteries because of several advantageous characteristics, including low density (0.534 g cm^{-3}), making them lightweight, and a perfect material for portable electronics. They are also known for their high specific capacity (3860 mAh g^{-1}) [19], making them a valuable material for batteries' electrical energy storage. It has a low redox potential (−3.04 V vs. SHE), which makes it an excellent choice for batteries due to its quick transfer of electrons during electrochemical reactions [13].

In early 1958, Harris studied the solubility of lithium in a range of non-aqueous electrolytes, including cyclic esters, molten salts, and inorganic lithium salt ($LiClO_4$) dissolved in propylene carbonate. During his investigation, he noticed the formation of a passivation layer capable of inhibiting a direct chemical interaction between lithium and the electrolyte while allowing for ionic transport, prompting more research into lithium-ion battery stability [18, 19]. These findings spurred an interest in the commercialization of primary LIBs. However, lithium-based batteries are subdivided into various subclasses, which include lithium-ion batteries (LIBs), lithium-sulfur (Li-S), and lithium-oxygen (Li-O_2) batteries [2].

2.2. Lithium-Sulfur Batteries (Li-S):

Lithium-sulfur batteries (Li-S) exhibit considerable potential for energy storage due to their low cost and high energy density. They are more environmentally friendly because they do not employ rare metals as cathode materials [20, 21]. A Li-S battery operates by coating a thin metalized substrate, like aluminum, with a porous sulfur composite cathode on a polymeric layer. During operation, soluble sulfur, and lithium polysulfides are produced at the cathode and diffused to the anode, where they participate in a parasitic reaction with the lithium to restore the low oxidation state of the polysulfides (Fig. 1). However, using electrolytes aids in increasing the capacity of Li-S batteries [16]. These electrolytes are manufactured using organic solvents combining dimethyl sulfide organics, diglyme, 1,3-dioxolane, 1,4-dioxane, 1,1-dimethoxyethane, glycol dimethyl ether, and lithium salts. Consequently, the negative electrode of a Li-S could consist of an alloy of calcium and lithium with a calcium atomic proportion ranging from 2% to 34%, which improves the battery performance [22, 23]. However, some challenges still need to be fixed in Li-S. Among these challenges are the poor conductivity of sulfur cathode materials, the dissolution and shuttle of polysulfides, and the volumetric expansion that occurs while charging and discharging [21, 24]. Various strategies have been studied to overcome these challenges. These include creating carbon-sulfur composites with different material structures to enhance the electrochemical performance, employing metal-based catalysts decorated-carbon materials to improve the electrochemical performance of Li-S batteries, and creating solid-state electrolytes (SSEs) to extend the safety and cycle life of Li-S batteries [25, 26]. However, Li-S batteries are a potential next-generation energy storage technology; nevertheless, more research is needed to resolve outstanding problems and improve their usefulness for practical applications [25, 26].

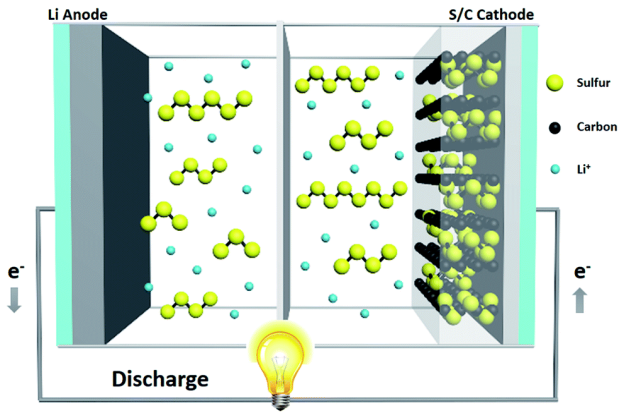

Fig. 1: Schematic description of the working principle of Li-S [27].

2.3. Lithium-oxygen (Li-O_2) Batteries

Lithium-oxygen (Li-O_2) batteries have garnered considerable interest because of their high energy theoretical density. Notwithstanding, they still have some challenges which depend on their design and composition. These challenges include irreversible lithium stripping or plating, reducing the battery's capacity [28], and the forming of the insulating and insoluble discharge product, lithium peroxide (Li_2O_2), which reduces battery performance [29]. Others include poor cycle stability and large discharge/charge overpotentials [30]. However, diverse approaches have been suggested to address these issues, and these include creating solid/solid interfaces to control Li_2O_2 development [31], employing solvation-regulated electrolytes to sustain the lithium anode [32], and creating catalysts to enhance the stability and electrochemical reactions in the battery. Another strategy is facilitating the direct 4e-catalytic reaction of LiOH in the storm by utilizing a metal-organic framework-derived catalyst, such as a single-atom Co-N_4/graphene catalyst [31]. An alternative method uses an engineered organic compound as a superoxide radical quencher and redox mediator to create more easily decomposable Li_2O_2 nanoparticles [33]. Further, a soluble catalyst that permits the reversible cleavage/formation of O-O bonds, like a copper (I) complex, are added to modify the reaction paths of Li-O_2 batteries [34]. In addition, soluble redox mediators like iron phthalocyanine can be employed as transition metal phthalocyanines to regulate the redox potentials and activity in Li-O_2 batteries [34]. Nonetheless, these various strategies aim to extend the cycle life, energy efficiency, and discharge capacity of Li-O_2 batteries.

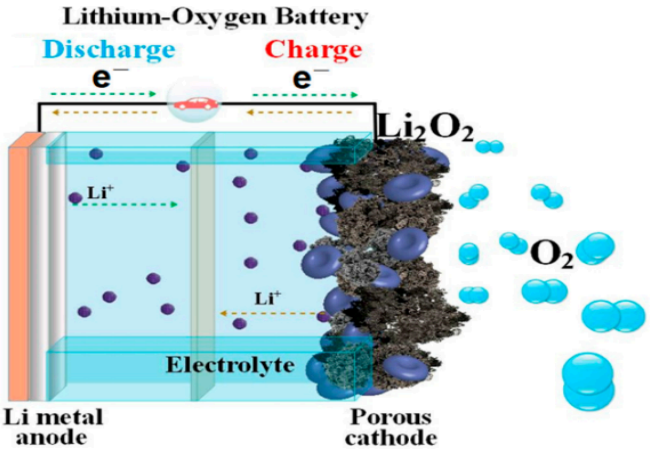

Fig. 2: Schematic description of the working principle of Li-O_2 [35].

2.4. Lithium-ion Batteries (LIBs)

LIBs have emerged as the most popular lithium-based battery system due to their high energy density, high voltage performance, low self-discharge, lack of memory effect, superior cycle performance, and strong rate performance [2]. Since 1991, LIBs have been widely employed in consumer mobile devices such as smartphones and laptop computers owing to their lightweight design and high-energy content [36]. The electrochemical performance of LIBs is determined by four major components: the anode, cathode, electrolyte, and separator [2]. The separator is a porous membrane that electrically separates the two electrodes. The negative electrodes (Anode) are primarily graphite and amorphous carbon compounds, while the positive electrode (cathode) consists of active materials such as mixed oxides. During charging and discharging, single lithium ions pass between the electrodes of LIBs, becoming intercalated in the active materials. Thus, electrons are released during discharge when lithium is deintercalated from the negative electrode. These are the materials via which lithium is intercalated [36].

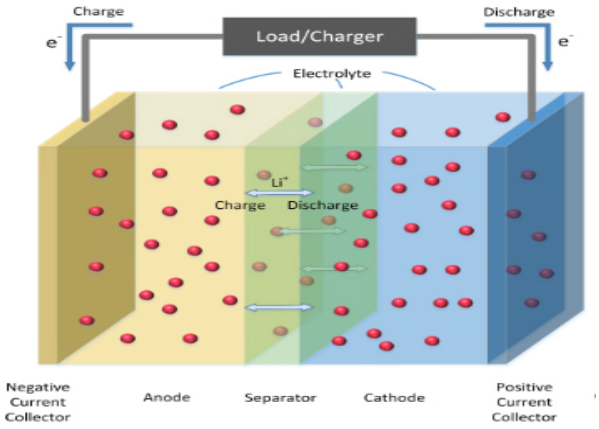

Fig. 3: Schematic description of the working principle of LIBs [37].

2.5. Comparison of Lithium-ion battery, Li-S and Li-O_2

LIBs are superior to Li-O_2 and Li-S in several ways. They require less expensive catalysts and are more efficient due to their greater theoretical specific capacity and good kinetics without breaking O-O bonds [38]. Li-S also attracts study interest because of its similar qualities to lithium and abundance. Still, LIBs are now considered state-of-the-art for large-scale energy storage [38 - 40]. LIBs are also widely utilized for various purposes, including electric cars and tiny electronic devices, and attempts are being made to make them more sustainable by using sustainable materials and manufacturing techniques. It has been discovered that LIBs are superior to the application of electric car batteries in terms of quality and capacity [39 - 40].

Comparing LIB to Li-O_2 and Li-S batteries, the former has greater capacity, efficiency, and sustainability. However, LIBs have issues that make it difficult for them to operate reliably, which include capacity limitation, low temperature, high positive overpotential, and poor cycle efficiency, among others [2]. Consequently, the challenges of low temperatures also lead to reduced cycle life, capacity loss, and security problems. The primary reasons for these issues include dendritic growth, low Li^+ diffusion coefficient, poor transfer kinetics, high Li^+ desolation barrier, and Li plating. The significant decrease in energy and power densities at low temperatures, caused mainly by interfacial charge transfer resistance, presents another difficulty. The twisted or broken ion routes inside and between solid components hinder cathode growth in

solid-state lithium metal batteries. Thus, LIBs short lifespan and inadequate capacity further hamper long-term operation and long-distance driving in electric vehicles [41 - 42].

2.6. Recent Development Lithium-based Batteries

The complexity of lithium-based batteries necessitates a multipronged strategy that involves international policy development supporting a circular economy for battery components, technological readiness, legal frameworks, upcycling and recycling procedures, and breakthroughs in logistics [41]. However, strategies have been implemented to help tackle the challenges in lithium-based batteries. Among these approaches, using anode and cathode materials with core-shell structure can enhance capacity performance and lengthen battery life [42]. Another innovative approach to addressing capacity degradation and safety concerns is using thermo-responsive separators in conjunction with intelligent self-protecting batteries, particularly in high-temperature environments [43]. Remedy options for low-temperature environments include optimizing charging processes, monitoring battery temperature in real-time, and improving intrinsic reactivity through intelligent cell design, surface coating, metal doping, morphology control, and particle size reduction for cathode modifications [44] have been used to solve these issues [35, 39]. However, problems still exist, with researchers identifying problems like voltage decay, capacity fading, and structural instability, especially with lithium cathode materials. Nevertheless, novel strategies involving manipulating MF materials have been investigated to overcome these difficulties [46]. This process emphasizes the continuous attempts to address complex problems and improve the efficiency and dependability of LIBs. It has demonstrated the potential to improve overall performance and stability, address issues related to low temperatures, and alter battery behavior.

In recent years, several researchers have focused on the effect of MF in lithium-based batteries, resulting in several novel and significant discoveries. Nevertheless, MF offers numerous advantages in Lithium-based batteries, including reducing the shuttle effect of small sulfur-containing molecules, decreasing Li dendrite formation, and increasing polysulfide capture. It can also help with problems including slow kinetics, electrode polarization, negative lithium dendrites, and poor catalytic performance of positive catalysts in Li-O_2 batteries [2, 5, 6, 17].

2.7. Magnetic Field

Based on existing research, historical magnetic theories, and analysis of the MF impact on the battery environment, the effect of the MF may be traced to five main factors: magnetic force, magnetohydrodynamic (MHD) effect, spin effect, magnetization, and nuclear magnetic resonance (NMR) [2]. However, the MHD effect, which characterizes the motion of a conductive fluid in the presence of an externally applied MF, is one of the most significant impacts when MF is applied to an electrochemical cell [17]. According to Shah Z. et al. [47], the MF interacts with the electric field as a non-contact method of transmitting energy in addition to the inherent magnetic force and magnetization properties. It is explained that the charged particles in an MF experience a Lorentz force because of the interaction between the electric and MF, which speeds up the electrochemical reaction and alters the initial direction of the flow of the charges. Thus, one innovative method currently gaining traction is using an MF to improve the electrochemical performance of batteries. However, more research on the technique is required [17, 48]. The benefits of MF and studies of physical phenomena resulting from magnetic interactions are applied in several battery situations. For instance, the idea of magnetic batteries, which included a helical spring strung into a magnetic core, was patented in 1987 by Ridley and Spector [17]. Further, the research of Hinds et al. [46] examined how MFs affected aqueous electrolytes, and nearly 100% of the electrochemical mass transport enhancement was shown when MF of 1 T was introduced to aqueous electrolytes. Costa et al. [41] assessed how an applied MF affected an electrochemical cell's ability to function to tackle the primary physical processes that may impact battery performance. They demonstrated that the electrochemical performance of lithium-based batteries, such as lithium-ion, lithium-sulfur, and lithium-oxygen batteries (Fig. 4), can be significantly improved by applying MF. It was reported that using external MF during cycling can prevent the production of lithium dendrites, leading to stable cycling at high current densities and dendrite-free lithium deposition. Consequently, magnetic properties have been used to help understand LIB materials' electrical and atomic structure and how they relate to electrochemical performance.

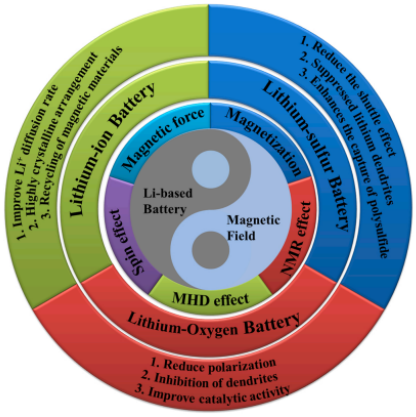

Fig. 4: Magnetic field application in lithium-based batteries (LIBs, Li-S batteries, and Li-O_2 batteries) and the five basic mechanisms involved [2]**.**

2.8. Magnetic Field Operation

The physical phenomenon known as magnetism, which dates back to the third century BC, is closely related to the development of our industrial civilization and daily lives. Faraday developed the electromagnetic induction phenomenon, which is the foundation of electromagnetism, while Oersted discovered the galvanomagnetic effect in the eighteenth century. However, from the eighteenth century to the present, there has been constant improvement in the theory of the metal electron, molecular MF, atomic magnetic moment, electron spin, magnetic domain, and other concepts. This approach has led to a theoretical understanding of magnetism that is comparatively comprehensive [2, 49], demonstrating that the movement of electric charges causes magnetic phenomena, with all macroscopic matter comprising atoms, fundamental building blocks of extranuclear electrons, and a nucleus. Because electrons are mobile, every atom has a magnetic moment, and due to this, magnetism is a fundamental characteristic of all materials, which are further categorized according to their magnetic properties, such as diamagnetic, paramagnetic, ferromagnetic, and antiferromagnetic [2, 17, 50].

2.8.1. Diamagnetic Material

Diamagnetic materials are minor repulsion when exposed to an MF. Diamagnetic materials do not contain unpaired electrons and are negatively magnetically sensitive. However, LIBs can operate at larger capacities due to diamagnetism. Thus, by altering the mass movement, electrolyte characteristics, electrode kinetics, and deposit morphology, MF can enhance the electrochemical processes in LIBs [2]. Nevertheless, new ideas and enhanced battery topologies could result from the interaction between magnetic forces and LIB components. Additionally, studies have looked at the application of solid-state nuclear magnetic resonance spectroscopy for solid-state lithium battery transport measurements and structural characterization. Notably, the potential for energy storage and LIB battery performance can be improved by comprehending and utilizing diamagnetism in LIB applications [2, 17].

2.8.2. Paramagnetic Material

Materials classified as paramagnetic have unpaired electrons, which cause them to be weakly attracted to an MF. They show signs of being positively magnetically susceptible and are affected by MF. It has been investigated how applying LIBs can enhance their performance due to their paramagnetic properties [2]. Consequently, by influencing electrochemical reactions, electrolyte characteristics, mass transportation, electrode kinetics, and deposit morphology, MF in LIBs can produce more inventive and high-performing battery architectures. Moreover, promising outcomes are also observed when one-dimensional metal-organic compounds are used as LIB electrode materials. These materials offer a new system for future research by keeping organic active compounds insoluble in the electrolyte throughout charging and discharging. Further, the creation of lithium dendrites during cycling has been suggested to be suppressed by external MF, which would enhance Li^+ diffusion and permit dendritic-free lithium deposition at high current densities. Thus, applying MF on paramagnetic materials may improve LIB's electrochemical performance and safety [17].

2.8.3. Ferromagnetic Material

Due to their intense attraction to MF, ferromagnetic materials can retain their magnetization even after the external MF is withdrawn. Ferromagnetic forces can improve LIB performance by influencing electrochemical reactions and other battery system components [2]. However, MF

has been used in lithium-based batteries to increase electrochemical performance using magnetic force, magnetization, magnetohydrodynamics, and spin effects. Notwithstanding, external MF can improve lithium metal batteries' stability and safety by preventing lithium dendrites' formation during cycling. Furthermore, the electrochemical performance of battery materials has been elucidated by utilizing magnetic properties related to charge and mass transfer, redox processes, and atomic details. As a result, ferromagnetic forces have shown promise for enhancing LIB performance and safety while shedding light on their underlying mechanics [17].

2.8.4. Antiferromagnetic Material

Antiferromagnetic is a form of magnetic ordering that occurs when adjacent magnetic moments align against one another, producing zero net magnetization. The magnetic moments of adjacent atoms or ions align antiparallel in antiferromagnetic materials, wiping out each one's distinct MF [46]. Consequently, antiferromagnetic materials do not show macroscopic magnetization because the magnetic moments cancel each other out. To create creative and high-performing battery designs, one must comprehend the magnetic properties of LIB. However, magnetic forces and interactions influence LIB's antiferromagnetic behavior. In $LiFePO_4$, where Fe^{2+} ions take the place of Li^+, magnetic moments at antisite defects result in quasifree [51] moments that are not involved in long-range antiferromagnetic order. These magnetic moments exhibit strong zero-field splitting and extremely anisotropic g factors because their anisotropy axes align with the principal crystallographic directions. The magnetic characteristics of lithium intercalation compounds can be studied, and magnetic studies can be used to assess the purity of the electrode materials used in rechargeable Li^+ batteries. Nevertheless, magnetic force, magnetization, magnetohydrodynamic, and spin effects can all be used to enhance the electrochemical performance of lithium-based batteries by applying a magnetic field [49, 51, 52].

2.9. Magnetic Field Effect

Numerous methods are outlined by which an MF controls electrochemical reactions (Fig. 5). However, acid-based materials and the Hall effect MFs applied and their impact on changes in electrical conductivity. MHD events interacting with the convective diffusion layer close to the

electrodes are primarily responsible for the MF superposition. Thus, MF-caused modifications to the electrode kinetics (also known as electrochemical kinetics). Morphological and qualitative changes in the deposit during magneto electrolysis [2, 17].

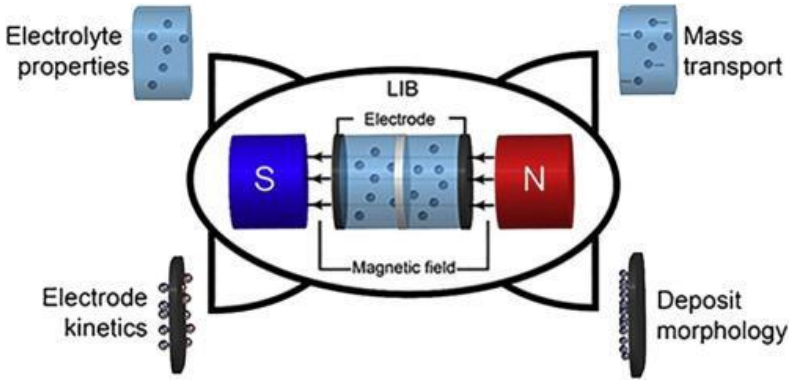

Fig. 5: Schematic illustration of the potential effects of an applied magnetic field on electrochemical reactions, particularly those involving a battery [17].

2.10. Magnetic Force

Magnetic domains exist in all materials. Thus, when an MF is applied to the magnetic domains, the magnetic poles move uniformly in one direction; when removed from some magnetic substances, the magnetic domains cannot return to their original principles. Permanent magnet materials are used to demonstrate magnetism. However, suppose the material magnetism decreases without an MF. In that case, such material is known as a soft magnetic substance, although all magnetic materials exhibit attraction between opposing MF and repulsion between aligned MF. Nevertheless, numerous research groups have applied this physical phenomenon to LIBs to avoid active material differentiation and failure, the polysulfide shuttle effect, and promote magnetic material recovery [2, 5, 17].

2.11. Magnetization Effect

Magnetism is created when a substance's magnetic moments line up in the presence of an MF; this process is called magnetization. However, a substance that is not inherently magnetized

can be made magnetized by applying an MF. Thus, by utilizing this method, the orientation of the crystal can be changed/enhanced to create an oriented crystal structure, which can improve lithium storage, making it easier for Li^+ to be transported. As seen in Fig. 6, the superparamagnetic zinc ferrite was magnetized and showed a typical configuration in an MF [2]. Numerous articles have examined the magnetization effect in LIB. Ameziane et al. demonstrated solid-state LIB technology for switching voltage-controlled in-plane and perpendicular magnetization states in a Co-Pt bilayer [53]. Further, to improve Li^+ diffusion and lessen the driving force for dendritic formations, Chen et al. [54] suggested employing external MF to prevent the production of lithium dendrites during cycling. Kimura et al. [55] performed magnetization and high-frequency electromagnetic spectrum (EMR) studies on lithium manganese spinel ($LiMn_2O_4$) powder samples. These investigations revealed differences in magnetization and EMR spectra between samples. Further, a LIB electrode plate with a groove in the active substance layer was studied. This process extended the cycle life and enhanced the high-magnification charge-discharge characteristic [5]. Li et al. [56] investigated the diffusion-polarization effect in LIB to lessen polarization effects and shorten test times, and they suggested a quick depolarization technique using pulse charge discharge.

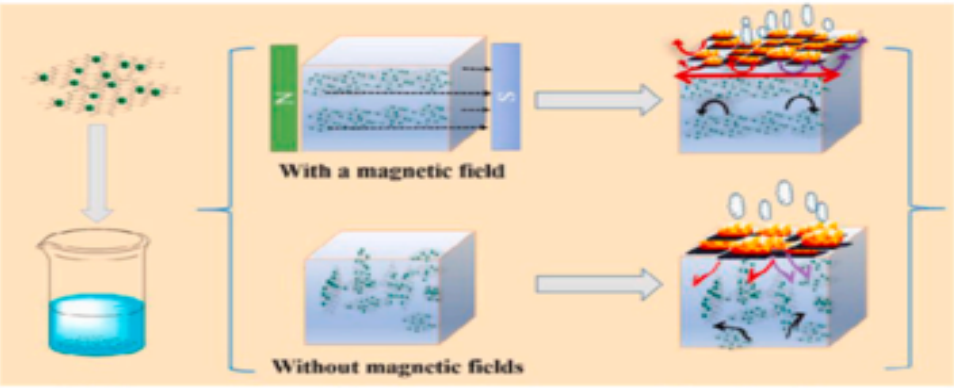

Fig. 6: Magnetic field magnetization: Zinc ferrite nanoparticles are magnetized into an ordered pattern in a magnetic field. Li+ is subjected to the Lorentz force in a magnetic field to produce the MHD effect [2].

2.12. Magnetohydrodynamic (MHD) effect

Applying an electrochemical reaction in an MF, the electromagnetic interaction induces convection in an electrolytic solution [57]. The charged species in the electrolyte experience a Lorentz force perpendicular to the electric and magnetic fields. This force alters the movement direction of charged species, forcing them to spiral and creating convection in the electrolyte, hence promoting mass transfer and the uniform distribution of Li^+ [57, 58]. For instance, during electrochemical deposition, the Lorentz force rotates the charged lithium ions, churning the electrolyte and enhancing mass transfer, improving electrode responsiveness. This also aids in the electro-crystallization process by enhancing the form and structure of the deposited Li^+ layer [58]. Further, the formula FL = j × B determines the Lorentz force, where j represents the local current density, and B represents the external MF intensity. The Lorentz force is 0 when B and j are parallel and greatest when orthogonal. At the electrode's edge, the direction of j twists and cuts off the magnetic force lines, causing the MHD process to generate eddy currents [57]. Furthermore, protrusions on the electrode surface affect the local current distribution, resulting in micro-MHD eddy currents (Fig. 7) [57]. The micro-MHD effect improves the concentration of polarized lithium ions while reducing dendrite formation [2, 59].

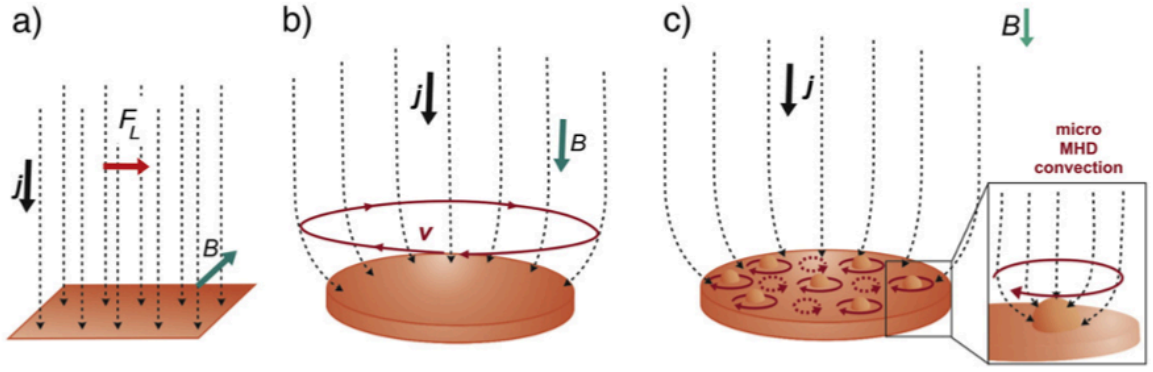

Fig. 7: The micro-MHD effect improves the concentration of polarized lithium ions while reducing dendrite formation [54].

2.13. Spin Effect

Recent research shows that MF has a substantial impact on spin-dependent electrochemistry. Figure 8 depicts a diagrammatic depiction of the spin effect. The figure shows that the MoS_2 catalyst lowers the energy barrier for electronic transitions under an MF, enhancing catalytic efficiency [60]. Thus, spin rules under MF circumstances are observed in electrochemical reactions, principally through the spin-related free radical pair mechanism and other mechanisms [61]. Spin-related radical pairs have a significant role in electrochemistry. As observed, MF causes the spin arrangement to shift from disordered to ordered, resulting in a change in surface energy, which can impact reactant adsorption, catalytic activity, and reaction activity [2]. Previous research has demonstrated that spin-aligned materials have a higher spin density on atoms than non-spin-aligned materials. This process implies that when exposed to a vertical MF, ferromagnetic materials are magnetically sensitive and absorb more energy [61]. This medium will increase the usefulness of magnetic materials in catalysis and Li-O_2 batteries [2].

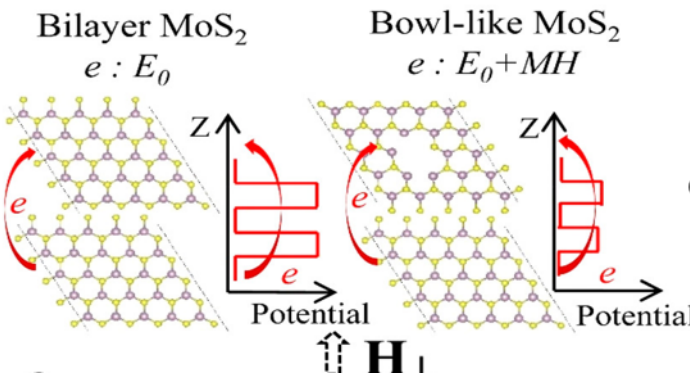

Fig. 8: Schematic of electron transfer in bilayer MoS_2 and bowl-like MoS_2 under an external magnetic field[60].

2.14. Magnetic Application in Lithium-ion Batteries: Material Synthesis

The anode, cathode, electrolyte, and separator determine LIB electrochemical performance. The electrode materials must be electrically and ionically conductive to allow for the reversible insertion and extraction of Li^+ across thousands of cycles [62, 63]. The cathode and anode materials must have a suitable lattice structure, crystallinity, and structural stability to meet the requirements of the rocking chair battery model [64]. The electrolyte conditions are primarily focused on ionic solid conductivity. Numerous investigations have shown that an MF can

produce ferromagnetic and paramagnetic materials with unique crystal structures [46]. When an MF is applied to a material's synthetic process, the nucleation and growth processes modify and cause anisotropy, impacting the crystal lattice alteration. This is due to decreased surface energy, increased directionality along the easy axis, and dipole enhancement [65]. Furthermore, the magnetic field-induced method is comparable to a strategy that does not use a template. An MF facilitates the production of electrode materials and electrolytes for Li^+ insertion/extraction [2, 17]. For instance, Zhou et al. [5] aligned $LiFePO_4$ monocrystalline platelets along the b-axis to enhance high-rate performance using a 0.5 T magnetic field, and this alignment increased the Li^+ diffusion coefficients, which boosted the capacity for rapid discharge (see Fig. 9). Cham Kim et al. [6] investigated the magnetism and magnetic susceptibility of $LiFePO_4$ using a 6 T superconducting magnet system. The aligned $LiFePO_4$ demonstrated lower electrode polarization and higher reversible capacity, implying the possibility of improved battery performance.

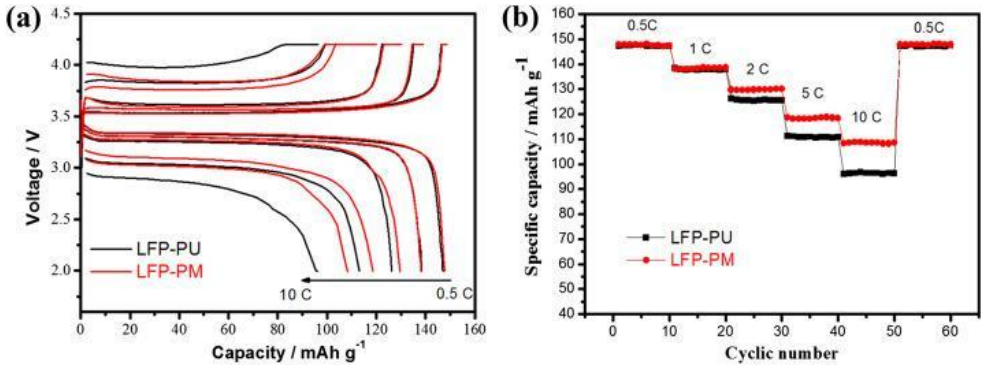

Fig. 9: Electrochemical performance of the LFP-PU and LFP-PM cathodes: (a) charge/discharge capacities, (b) rate performance [5]**.**

2.15. The use of Magnetic Nanoparticle to Enhance the Electrochemical Performance of LIBs

Magneto-sensitive materials (MNPs) have recently been studied to improve electrochemical and structural properties of electrodes in LIBs. As a result, research has been recently conducted into employing Fe_2O_3 as an MNPS to increase LIB electrochemical performance due to various benefits, including high theoretical capacity, non-toxicity, and strong corrosion resistance [14, 66]. However, Fe_2O_3 has limitations, such as significant irreversible capacity loss and low cycle

stability. Various solutions have addressed these restrictions [66 - 69]. Due to improved electrical conductivity, better redox reversibility, and shorter transit lengths for both Li^+ and electrons, α-Fe_2O_3 nanoparticles with electronically conductive coating layers are more effective at enhancing the battery's electrochemical capabilities [66]. For example, Liu et al. [14] used Fe_2O_3 to create a $LiFePO_4$/C cathode material with high-capacity retention and reversibility (145.8 $mAhg^{-1}$ at 0.2 C). Wang et al. [12] created $LiFePO_4$/C composites by heating Fe_2O_3 to 600 °C, and the most excellent discharge capacity (156 $mAhg^{-1}$) was attained at 0.1 C using sucrose as a carbon source. Ho-ming et al. [15] employed γ- Fe_2O_3 to manufacture a $LiFePO_4$ cathode in a magnetic field. The $LiFePO_4$ electrode, containing 15% γ- Fe_2O_3, outperforms the pure $LiFePO_4$ electrode with a discharge capacity of 69.8 mAh-1 at 10 C due to the MF it creates. These results show that incorporating Fe_2O_3 into the electrode is a simple and inexpensive method for boosting LIB power density and cycle life.

3.0. Chapter Three – Materials and Method

The method employed for this study will be subdivided into the following.

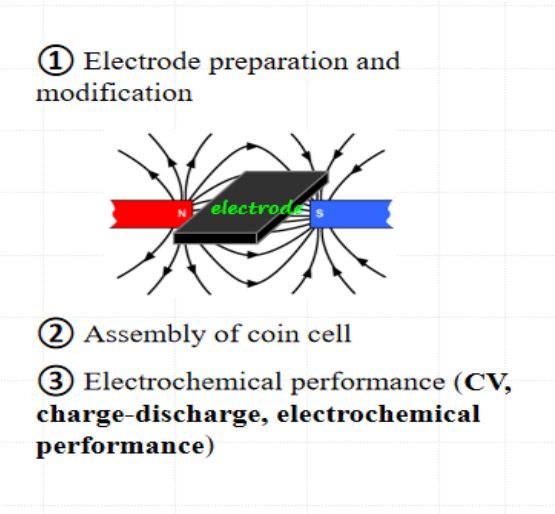

Fig. 10: Method Description.

3.1. Chemicals and Instruments

The active material was commercial $LiFePO_4$, the conductive substance was acetylene black with Nw = 150G, the MNP was iron (III) oxide (Fe_2O_3), and the binder was Poly (vinylidene fluoride) (PVDF) with Mw = 1100 kg/mol (All chemicals were purchased from MTI corporation, 860 S. 19th Street, Richmond, CA) N-Methyl 2-pyrrolidone (NMP) was used as the solvent, and its purity was 99.8%. To decrease residual moisture content, the active, PVDF, and conductive components were post-dried in a vacuum oven at 60 °C for 12 hours before slurry production.

3.2. Sample Characterization

The crystal and phase structures of the as-prepared LiFePo4 cathode materials were characterized by X-ray diffraction (XRD, Smart Lab. Co, Japan) with Cu Kα radiation (λ = 0.154056 nm). The samples were scanned at diffraction angles ranging from 10 to 70° at 1° per minute, 40 KV, and 15 mA. Scanning electron microscopy (SEM, JSM, -7500F JEOL, Japan) was used to examine sample particle size and shape.

3.3. Cathode Preparation

The cathode slurry contains 80:10:10, 80:10:9:1, and 80:10:7:3 (all in wt%), which were prepared in a 600 µl n-methyl pyrrolidone solvent (NMP). A planetary centrifugal vacuum mixer (ARV-310CE, Iwamoto-Cho Chiyoda-Ku, Tokyo, Japan) was used to mix the slurries. The planetary mixer spins the sample holder's axis in the opposite direction while rotating the samples around a central axis; each cycle was centrifuged for 15 minutes at 1200 rpm and 98.2 kPA. The samples were mixed twice (30 minutes) to evenly distribute the solvent, binder, active material, Fe_2O_3, and conductive components. The homogeneous slurry was coated on an aluminum current collector with a 20 µm doctor blade, placed on an MF of 0.3 T, and dried at 60°C under vacuum for 6 hours to form a directionally dispersed cathode, abbreviated LFP-MF, LFP+1 wt% Fe_2O_3-MF, and LFP+3 wt% Fe_2O_3-MF. In contrast, a homogeneous slurry was dried without a magnetic field (WMF), resulting in a naturally distributed LFP-WMF, LFP+1 wt% Fe_2O_3-WMF, and LFP+3 wt% Fe_2O_3-WMF cathodes.

Table 1. Protocol for Cathode Slurry Preparation

Active material	Conductive material	Binder	Magnet sensitive material	Slurry compositions	Solvent	Denote
$LiFePO_4$	Acetylene black	PVDF		80:10:10	NMP	LFP-WMF
$LiFePO_4$	Acetylene black	PVDF		80:10:10	NMP	LFP-MF
$LiFePO_4$	Acetylene black	PVDF	Fe_2O_3	80:9:10:1	NMP	LFP + 1 wt% Fe_2O_3 -WMF
$LiFePO_4$	Acetylene black	PVDF	Fe_2O_3	80:9:10:1	NMP	LFP + 1 wt% Fe_2O_3 -MF
$LiFePO_4$	Acetylene black	PVDF	Fe_2O_3	80:7:10:3	NMP	LFP + 3 wt% Fe_2O_3 -WMF
$LiFePO_4$	Acetylene black	PVDF	Fe_2O_3	80:7:10:3	NMP	LFP + 3 wt% Fe_2O_3 -WMF

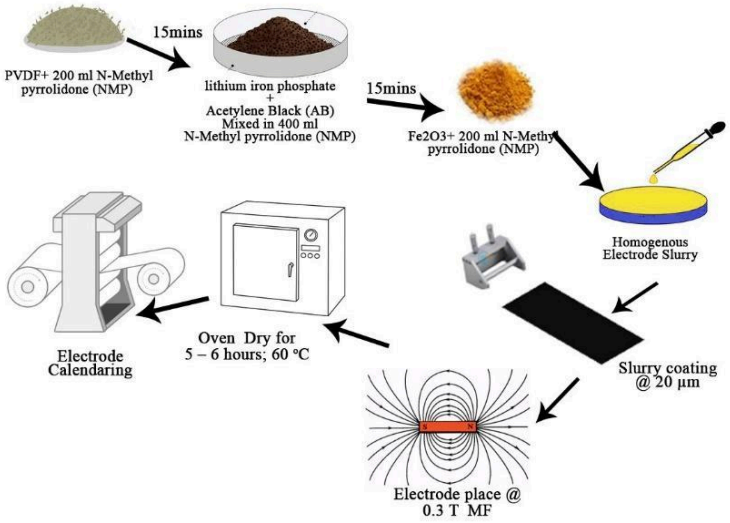

Fig. 11: Experimental (Cathode Preparation Process).

3.4. Assembling process and electrochemical performance test

The dry cathodes were roll-pressed on a calendaring machine (Non-heating WCRP-1015G, Hohsen, Corp.) and punched into 14 mm-diameter platelets. Coin-type cells (CR2032) were used

to test the electrodes' electrochemical properties in a glovebox with a dry Argon environment (0.1 ppm of oxygen and water). The separator and electrolyte were a polypropylene membrane (Celgard 2400) and 1 M $LiPF_6$ in DMC: EC (1:1 v/v), with a lithium chip as the anode electrode. To determine the diffusion coefficient of the $LiFePO_4$ cathode, cyclic voltammogram (CV) measurements were performed at room temperature on a Biologic tester (VMP3 s/n: 0726, 264 Argyll Avenue, France) at varied scan speeds ranging from 0.1 to 0.5 mVs^{-1}, and a voltage ranging from 2.8 to 4.2 V. Galvanostatic charge/discharge experiments were carried out using a Neware Battery Test System (China) at charge-discharge rate ranging from 0.1 C to 5 C and working voltages ranging from 4.2 to 2.8 V. Electrochemical impedance spectroscopy (EIS) was performed using a Biologic Inc. workstation (VMP3) with a frequency range of 100 kHz to 0.1 Hz and amplitude of 10 mV.

4.0. Chapter Four – Result and Discussion

4.1. Material Characterization via XRD

XRD was used to analyze the crystalline properties of the $LiFePO_4$ powder and related cathodes, both with and without magnetic placement. The sample's diffraction peaks fit the $LiFePO_4$ standard pattern, and the absence of additional peaks indicates that the samples included few to no other crystal impurities. All LFP-MF and LFP-WMF (Fig. 12 (a)); LFP+1 wt% Fe_2O_3-MF and LFP+1 wt% Fe_2O_3-WMF (Fig. 12 (b)); LFP+3 wt% Fe_2O_3-WMF and LFP+3 wt% Fe_2O_3-MF (Fig. 12 (c)) diffraction peaks can be indexed to an orthorhombic Pnma space group matching to the standard data (JCPDS card no. 01-090-1862). However, due to the high intensity of the $LiFePO_4$ powder crystal peaks, it is tough to discern the amorphous peaks of PVDF, acetylene black, and Fe_2O_3 in the cathodes.

4.2. Material Characterization via SEM

The morphology of the $LiFePO_4$ powder and the influence of MF on the positive electrode thickness were investigated using SEM; Fig.13 shows SEM images of the $LiFePO_4$ powder and the corresponding electrodes, while Fig. 14 shows the cross-sectional SEM images of the $LiFePO_4$ positive electrode on MF and WMF. As shown in Fig 14 (a) and (b), the SEM cross-sectional images of electrodes reveal cathode thickness for LFP-WMF (17.64 µm) and LFP-MF (15.63 µm). Fig. 14 (c) and (c) show the thickness of LFP+1 wt% Fe_2O_3-WMF (16.97 µm) and LFP+1 wt% Fe_2O_3-MF (14.40 µm) electrodes, while Fig. 14 (e) and (f) revealed the cathode thickness of LFP+3 wt% Fe_2O_3-WMF (17.20 µm) and LFP+3 wt% Fe_2O_3-MF (15.97 µm). Based on the results obtained, it was observed that the MF treatment influences cathode thickness.

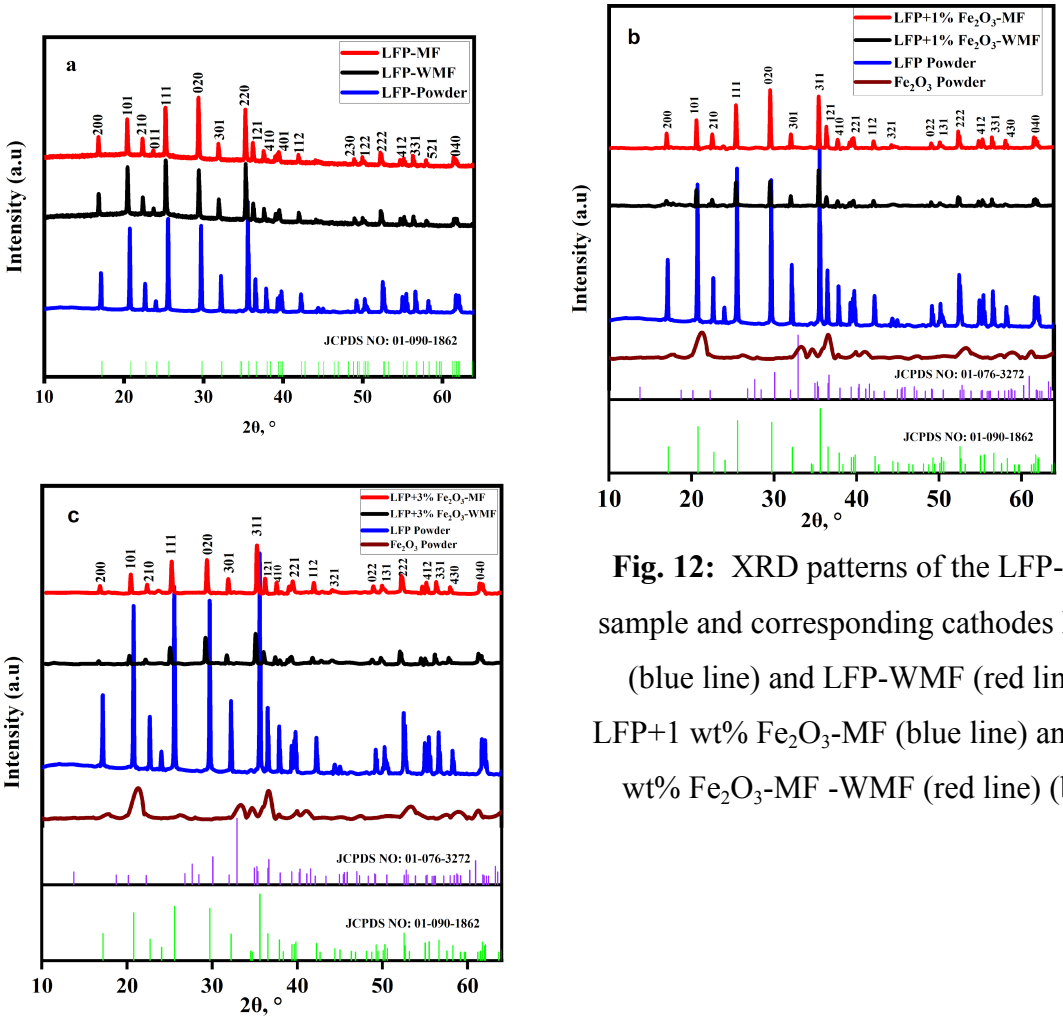

Fig. 12: XRD patterns of the LFP-powder sample and corresponding cathodes LFP-MF (blue line) and LFP-WMF (red line) (a); LFP+1 wt% Fe_2O_3-MF (blue line) and LFP+1 wt% Fe_2O_3-MF -WMF (red line) (b); and

LFP+3 wt% Fe_2O_3-MF (blue line) and LFP+3 wt% Fe_2O_3-MF -WMF (red line) (c).

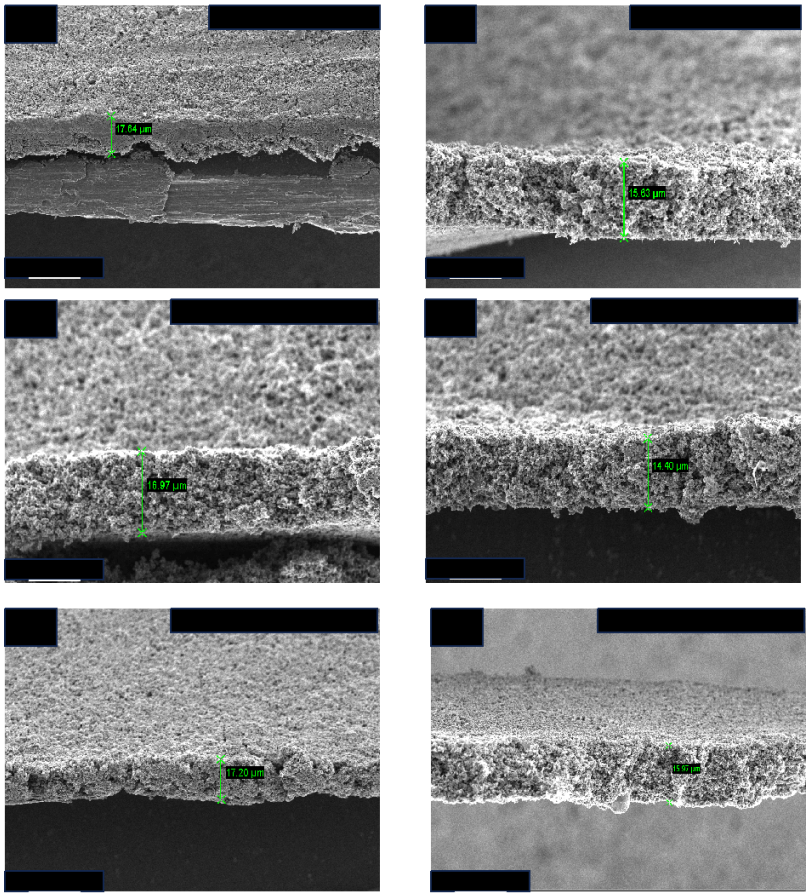

Fig. 13: The cross-sectional SEM images of the $LiFePO_4$ cathode electrode: LFP-WMF and LFP-MF (a) and (b); LFP+1 wt% Fe_2O_3-WMF and LFP+1 wt% Fe_2O_3-MMF (c) and (d); and Fig. LFP+3 wt% Fe_2O_3-WMF, and LFP+3 wt% Fe_2O_3-WMF (e) and (f).

Fig. 14 (a) and (b) depict an SEM image of $LiFePO_4$ powder. The image shows that the $LiFePO_4$ powder sample has spherical particles with evenly dispersed grains. According to [11], a single particle with a particle size below 2.5 μm enables magnetic orientation when exposed to an external MF. Thus, the $LiFePO_4$ sample is micro-sized, measuring 100-699.2 nm (0.1-0.70 μm) in length, and as such, it needs a small MF strength to affect the particle orientation [5]. Further, Fig. 14 (c) and (d) show the top-view SEM image of LFP-WMF and LFP-MF cathodes,

(e) and (f) show for LFP+1 wt% Fe_2O_3-WMF and LFP+1 wt% Fe_2O_3-MF cathodes, and Fig. 14 (g) and (h) show the top-view SEM image for LFP+3 wt% Fe_2O_3-WMF and LFP+3 wt% Fe_2O_3-MF cathodes. As shown in the figures, the composite powder was well-mixed with carbon. However, no effect could be observed for all electrodes with MF and WMF, as all $LiFePO_4$ particles on the electrodes were randomly distributed and cannot be distinguished from each other at the 1 μm scale bar images. At the 50 μm scale bar pictures, the $LiFePO_4$ powder samples could hardly be observed due to the binder and the carbon covering the surface of the electrode.

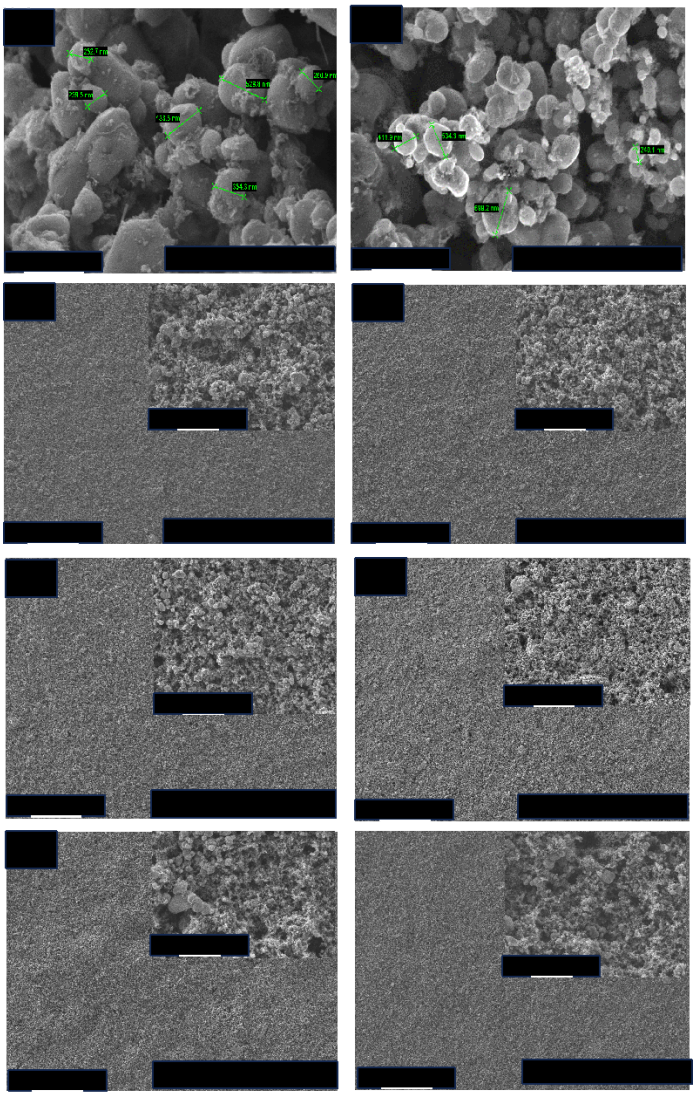

Fig. 14: SEM images: $LiFePO_4$ powder sample (a) and (b); LFP-WMF and LFP-MF (c) and (d); LFP+1 wt% Fe_2O_3-WMF and LFP+1 wt% Fe_2O_3-MF (e) and (f); and LFP+3 wt% Fe_2O_3-WMF, and LFP+3 wt% Fe_2O_3-WMF (g) and (h)**.**

4.3. Cyclic Voltammetry (CV)

CV experiments were performed to investigate the MF effect on the electrode operation. The potential differences (ΔV) between the oxidation and reduction peaks [5, 11] were calculated to evaluate the polarization variation due to the magnetic field effect. All electrodes (MF and WMF) displayed distinct redox peaks (Fig. 15), correlating to the electrochemical transformation of $Fe^{2+/}Fe^{3+}$ phases [6, 71, 72], indicating reversible Li^+ extraction and insertion processes. LFP-MF, LFP+1 wt% Fe_2O_3-MF, and LFP+3 wt% Fe_2O_3-MF electrodes exhibit notable anodic peaks at 3.53, 3.52, and 3.58 V (*vs. Li/Li*$^+$ for all electrochemical measurement) and cathodic peaks around 3.34, 3.33, and 3.29 V, and exhibiting a current difference of 1.57, 1.92, and 1.64 mA, respectively. The cathodic and anodic peak difference (ΔV) of the electrodes, which also reflects the kinetic polarization upon REDOX processes, in this case were 0.19, 0.18, and 0.29 V, respectively, which is lower compared to that of LFP-WMF (0.20 V), LFP+1 wt% Fe_2O_3-WMF (0.22 V), and LFP+3 wt% Fe_2O_3-WMF (0.36 V). The prominent anodic peaks of LFP-WMF, LFP+1 wt% Fe_2O_3-WMF, and LFP+3 wt% Fe_2O_3-WMF occurred at 3.54, 3.55, and 3.61 V, while the cathodic peaks occurred at 3.34, 3.33, 3.25 V with current differences of 1.15, 1.56, and 1.49 mA. It should be noted that a lower ΔV indicates better reversibility and enhanced electrode kinetics (lower electrochemical polarization) [5]. Thus, these results imply that the electrodes dried under MF exhibit improved electrode kinetics, reversibility, and slower capacity deterioration during long-term cycling, as shown later, while also exhibiting higher current (which reflects the reaction rate) values compared to all the electrode-prepared without subjecting to the magnetic field (WMF). This indicates that the cathodes placed on the MF possess better electrochemical performance in lithium batteries, which helps to enhance the rate capability of the cells as well [5, 6, 11].

Fig. 15: Comparison of CV data for LFP-WMF (black line) and LFP-MF (red line) (a); LFP + 1 wt% Fe_2O_3-WMF (black line) and LFP + 1 wt% Fe_2O_3-MF (red line) (b); and LFP + 3 wt% Fe_2O_3-WMF (black line) and LFP + 3 wt% Fe_2O_3-MF (red line) (c).

4.4. Diffusion Coefficient

Following evidence of MF's effects on the electrode by CV, the diffusion coefficient for the studied systems was estimated to confirm the impact of magnetic field on this. A high Li^+ diffusion coefficient is critical for a Li-ion battery's fast kinetics and electrochemical efficiency. The diffusion coefficient estimation was studied by CV at a scan rate ranging from 0.5 to 0.1 mVs^{-1} and was used to investigate the intrinsic kinetics of Li^+ interactions. Notably, as the scan rates increase, distinct redox peaks arise in the CV profiles of the electrodes (Fig. 16). When the scan rate increases, the reaction current increases, indicating a rise in the electrochemical reaction rate. At the same time, the redox peaks potential difference (between the oxidation and reduction peaks in the CV curves) also increases, showing that the electrode polarization rises. However, all the electrodes dried under MF exhibited superior electrochemical properties and higher lithium diffusion coefficients than the WMF electrodes.

Fig. 16: CV curves date for LFP-WMF (a), LFP-MF (b), LFP + 1 wt% Fe_2O_3-WMF (c), LFP + 1 wt% Fe_2O_3-MF (d), and LFP + 3 wt% Fe_2O_3-WMF (e), LFP + 1 wt% Fe_2O_3-MF (f), at different scan rates.

The Li^+ diffusion coefficients for all electrodes are shown in Table 2. As a result, the higher Li^+ diffusion coefficients of the electrodes dried under MF can be attributed to the magnetic field effect on the electrode materials' properties.

Table 2. Li^+ diffusion coefficients and the charge-transfer resistance (R2) Fitting values for LFP-MF, LFP-WMF, LFP+1 wt% Fe_2O_3-WMF, LFP+1 wt% Fe_2O_3-MF, LFP+3 wt% Fe_2O_3-WMF, and LFP+3 wt% Fe_2O_3-MF.

Sample	cm^2S^{-1}	R2
LFP-WMF	2.1430×10^{-4}	35.79 Ohm
LFP-MF	4.1376×10^{-4}	31.44 Ohm
LFP+1 wt% Fe_2O_3-WMF	2.4493×10^{-4}	20.52 Ohm
LFP+1 wt% Fe_2O_3-MF	4.0614×10^{-4}	18.64 Ohm
LFP+3 wt% Fe_2O_3-WMF	1.3189×10^{-4}	45.51 Ohm
LFP+3 wt% Fe_2O_3-WMF	2.3021×10^{-4}	30.40 Ohm

4.5. Galvanostatic cycling at 0.1 C and 0.2 C

The galvanostatic charge-discharge performance of the cathodes was assessed to thoroughly investigate the active materials' electrochemical behavior and the effect of the magnetic field. Fig. 17 depicts charge-discharge profiles for all electrodes at 0.1 and 0.2 C rates and a 4.2–2.8 V cutoff voltage for the 4th cycle. The 4^{th} cycle was chosen because the cell performance stabilizes during the initial cycles. According to the data, the discharge-specific capacity for LFP-WMF, LFP+1 wt% Fe_2O_3-WMF, and LFP+3 wt% Fe_2O_3-WMF at 0.1 C was 150.26, 148.85, and 144.38 $mAhg^{-1}$, respectively, which is lower than that for LFP-MF (152.03 $mAhg^{-1}$), LFP+1 wt% Fe_2O_3-MF (150.04 $mAhg^{-1}$), and LFP+1 wt% Fe_2O_3-MF (148.67 $mAhg^{-1}$). When the cycling rate was increased to 0.2 C, the discharge capacities for the MF dried electrodes were at 147.77, 149.24, and 142.42 $mAhg^{-1}$, respectively, which is higher than that of the WMF electrodes, 143.18, 144.24, and 139.67 mAhg-1, respectively. The findings imply that introducing an MF during the cathode drying process can help enhance the Li^+ ion diffusion, increase the discharge capacity, and improve the $LiFePO_4$ discharge capacity retention performance.

Fig. 17: Comparison data for charge-Discharge of LFP-WMF and LFP-MF at 0.1 C at 4th cycle (a); LFP-WMF and LFP-MF at 0.2 C (b); LFP + 1 wt% Fe_2O_3-WMF and LFP + 1 wt% Fe_2O_3-MF at 0.1 C (c); LFP + 1 wt% Fe_2O_3-WMF and LFP + 1 wt% Fe_2O_3-MF at 0.2 C (d); LFP + 3 wt% Fe_2O_3-WMF and LFP + 3 wt% Fe_2O_3-MF at 0.1 C (e); and LFP + 3 wt% Fe_2O_3-WMF and LFP + 3 wt% Fe_2O_3-MF at 0.2 C (f)

4.6. Rate Capability Tests

The electrochemical performance of $LiFePO_4$ electrodes was also investigated at varying C rates (Fig. 18). All electrodes dried under MF had higher reversible capacity and a slower capacity degradation compared to the WMF electrode. Furthermore, as the charge-discharge rate rises, the capacity of the cathode electrodes falls due to the kinetics limitations. As a result, LFP electrodes dried on MF accelerated Li^+ diffusion, accompanied by increased discharge capacities at high rates. However, at higher rates, the effect of MF becomes more apparent. At 1 C, the discharge capacities of LFP-MF, LFP+1 wt% Fe_2O_3-MF, and LFP+3 wt% Fe_2O_3-MF were 125.92, 132.48, and 130.94 $mAhg^{-1}$, respectively, which were higher than LFP-WMF (115.30 $mAhg^{-1}$), LFP+1 wt% Fe_2O_3-WMF (123.80 $mAhg^{-1}$), and LFP+3 wt% Fe_2O_3-WMF (123.08 $mAhg^{-1}$). At 2 C, the capacities of LFP-MF (113.26 $mAhg^{-1}$), LFP+1 wt% Fe_2O_3-MF (120.01 $mAhg^{-1}$), and LFP+3 wt% Fe_2O_3-MF (118.33 $mAhg^{-1}$), were higher when compared to LFP-WMF, LFP+1 wt% Fe_2O_3-WMF, and LFP+3 wt% Fe_2O_3-WMF (103.67, 110.41, and 109.84 $mAhg^{-1}$, respectively). Finally, at 5 C, the discharge-specific capacities of LFP-MF, LFP+1 wt% Fe_2O_3-MF, and LFP+3 wt% Fe_2O_3-MF were 93.58, 101.29, and 75.96 $mAhg^{-1}$, and are higher when compared to LFP-WMF (84.57 $mAhg^{-1}$), LFP+1 wt% Fe_2O_3-WMF (88.73 $mAhg^{-1}$), and LFP+3 wt% Fe_2O_3-WMF (65.69 $mAhg^{-1}$). However, compared to bare LFP without magnetic sensitive nanoparticles and LFP+3 wt% Fe_2O_3, the LFP+1 wt% Fe_2O_3 cathode performs better than others regarding discharge capacity.

Fig. 18: Comparison of LFP-MF (red line) and LFP-WMF (black line) (a); LFP + 1 wt% Fe_2O_3-WMF (black line) and LFP + 1 wt% Fe_2O_3-MF (red line) (b); and LFP + 3 wt% Fe_2O_3-WMF (black line) and LFP + 3 wt% Fe_2O_3-MF (red line) (c) for different C-rate**.**

4.7. AC Electrochemical Impedance Spectroscopy (EIS)

EIS analysis was utilized to assess the effect of MF on the charge transfer resistance of the electrodes. Fig. 19 shows the Nyquist plots for all cathodes after the 5th CV cycle at 0.1 mVs^{-1}. All ac impedance curves comprise two semicircles in the high to medium-frequency range and a straight line in the low-frequency zone. The semicircles feature a high-frequency intercept, representing the electrolyte's ionic conductivity. The equivalent circuit shows that R1 and Q could be responsible for the first semicircle in the high-medium frequency region. Where R1 represents the particle-to-particle and particle-to-collector contact resistances; R2 represents the charge-transfer resistance between the electrolyte and the active material; Q represents the CPE (constant phase element); and W represents the Warburg impedance (Zw), which could be attributed primarily to Li^+ diffusion in the bulk electrode [5, 6]. Consequently, Table 2 above presents the same circuit's critical fitting parameters (R2). As a result, all cathodes dried under MF exhibited lower charge transfer resistances compared to the WMF cathode. Thus, the circuit's total resistance is primarily determined by the sum of R2 and R1. Notwithstanding, LFP-MF, LFP+1 wt% Fe_2O_3-MF, and LFP + 3 wt% Fe_2O_3-MF display lower resistance/impedance and polarization in their conductive behavior than LFP-WMF, LFP+1 wt% Fe_2O_3-WMF, and LFP+3 wt% Fe_2O_3-WMF as seen in Fig. 19.

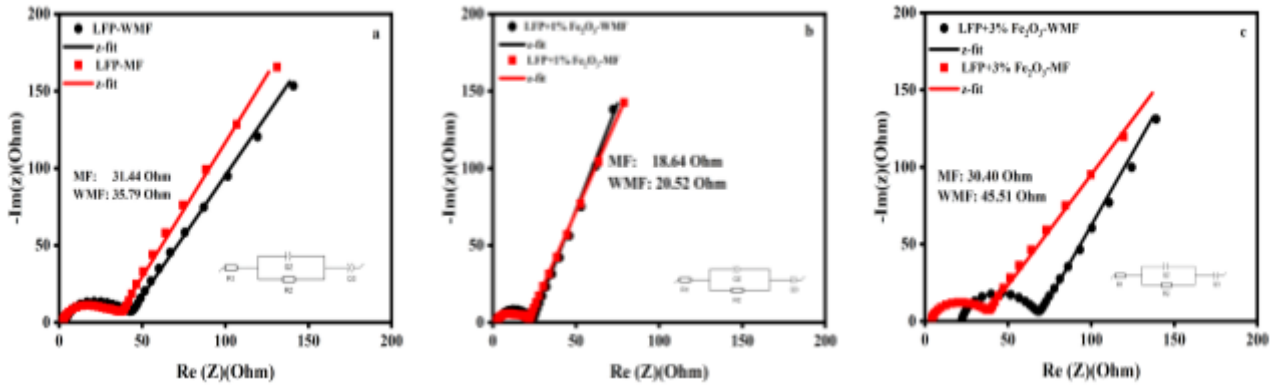

Fig. 19: Nyquist plots of ac impedance spectra data for LFP-WMF (black line) and LFP-MF (red line) (a); LFP + 1 wt% Fe_2O_3-WMF (black line) and LFP + 1 wt% Fe_2O_3-MF (red line) (b); and LFP + 3 wt% Fe_2O_3-WMF (black line) and LFP + 3 wt% Fe_2O_3-MF (red line) (c).

5.0. Chapter Five – Conclusion

In this study, commercial $LiFePO_4$ and Fe_2O_3 powder were mixed in three ratios to prepare composite cathodes using MF of 0.3 T during the preparation/drying process. According to the results obtained from the electrochemical test, the electrodes placed on the MF showed improved electrochemical characteristics in the material and suppressed polarization, thus contributing to better battery electrochemical performance. The discharge capacities for LFP-MF (147.77 $mAhg^{-1}$), LFP+1 wt% Fe_2O_3-MF (149.24 $mAhg^{-1}$), and LFP+3 wt% Fe_2O_3-MF (142.42 $mAhg^{-1}$) were superior at 0.2 C when compared to $LiFePO_4$ electrodes WMF and at a current density of 5 C, LFP-MF, LFP+1 wt% Fe_2O_3-MF, and LFP+3 wt% Fe_2O_3-MF maintained high capacities of 93.58, 101.29, and 75.96 $mAhg^{-1}$, respectively, surpassing those of the electrode WMF. Notably, the LFP-MF ($4.1376 \times 10^{-4}\ cm^2S^{-1}$), LFP+1 wt% Fe_2O_3-MF ($4.0614 \times 10^{-4}\ cm^2S^{-1}$), and LFP+3 wt% Fe_2O_3-MF ($2.3021 \times 10^{-4}\ cm^2S^{-1}$) exhibited an increased lithium-ion diffusion coefficient when compared to $LiFePO_4$ cathodes without MF. Based on the ac EIS result obtained, LFP-MF, LFP+1 wt% Fe_2O_3-MF, and LFP+3 wt% Fe_2O_3-MF show a lower charge transfer resistance of R2: 31.44, 18.64, and 30.40 Ohm compared to LFP-WMF (35.79 Ohm), LFP+1 wt% Fe_2O_3-WMF (20.52 Ohm), and LFP+3 wt% Fe_2O_3-WMF (45.51 Ohm). These advantages of using MF during the electrode preparation positively affected the material's electrochemical performance. Using MF to boost lithium-ion diffusion and whole electrochemical reaction in $LiFePO_4$ resulted in excellent reversibility and increased discharge capacities and stabilities at high cycling rates.

References:

[1] W. Zhao, "A forum on batteries: From lithium-ion to the next generation," *National Science Review*, vol. 7, no. 7. Oxford University Press, pp. 1263–1268, 2020. doi: 10.1093/NSR/NWAA068.

[2] K. Shen, X. Xu, and Y. Tang, "Recent progress of magnetic field application in lithium-based batteries," *Nano Energy*, vol. 92. Elsevier Ltd, February 1, 2022. doi: 10.1016/j.nanoen.2021.106703.

[3] B. Liu, J. G. Zhang, and W. Xu, "Advancing Lithium Metal Batteries," *Joule*, vol. 2, no. 5. Cell Press, pp. 833–845, May 16, 2018. doi: 10.1016/j.joule.2018.03.008.

[4] M. F. Lagadec, R. Zahn, and V. Wood, "Characterization and performance evaluation of lithium-ion battery separators," *Nature Energy*, vol. 4, no. 1. Nature Publishing Group, pp. 16–25, Jan. 01, 2019. doi: 10.1038/s41560-018-0295-9.

[5] J. Zhou, D. Zhang, G. Sun, and C. Chang, "B-axis oriented alignment of LiFePO4 monocrystalline platelets by magnetic orientation for a high-performance lithium-ion battery," *Solid State Ion*, vol. 338, pp. 96–102, Oct. 2019, doi: 10.1016/j.ssi.2019.05.002.

[6] C. Kim, Y. Yang, D. Ha, D. H. Kim, and H. Kim, "Crystal alignment of a LiFePO4 cathode material for lithium-ion batteries using its magnetic properties," *RSC Adv*, vol. 9, no. 55, pp. 31936–31942, 2019, doi: 10.1039/c9ra05284d.

[7] Y. Huang, C. fa Xiao, Q. lin Huang, H. Liang Liu, J. Qiang Hao, and L. Song, "Magnetic field induced orderly arrangement of Fe3O4/GO composite particles for preparation of Fe3O4/GO/PVDF membrane," *J Memb Sci*, vol. 548, pp. 184–193, Feb. 2018, doi: 10.1016/j.memsci.2017.11.027.

[8] "Advanced Energy Materials - 2019 - Li - Battery Electrodes Fabrication of Low‐Tortuosity Ultrahigh‐Area‐Capacity Battery".

[9] N. A. Chernova, G. M. Nolis, F. O. Omenya, H. Zhou, Z. Li, and M. S. Whittingham, "What can we learn about battery materials from their magnetic properties?," *J Mater Chem*, vol. 21, no. 27, pp. 9865–9875, Jul. 2011, doi: 10.1039/c1jm00024a.

[10] J. Guo *et al.*, "Enhanced saturation magnetization in buckypaper-films of thin walled carbon nanostructures filled with Fe3C, FeCo, FeNi, CoNi, Co and Ni crystals: the key role of Cl," *Physical Chemistry Chemical Physics*, vol. 17, no. 27, pp. 18159–18166, Jul. 2015, doi: 10.1039/c5cp02425k.

[11] D. Gao, J. Yang, D. Zhang, and C. Chang, "An effective strategy to enhance the electrochemical performance of LiNi0.6Mn0.2Co0.2O2: Optimizing a Li diffusion pathway via magnetic

alignment of single-crystal cathode material under an ordinary 0.4-T magnetic field," *Ceram Int*, 2022, doi: 10.1016/j.ceramint.2022.07.081.

[12] Y. Wang, H. Li, M. Chen, X. Yang, and D. Jiang, "Synthesis and electrochemical performance of LiFePO4/C cathode materials from Fe2O3 for high-power lithium-ion batteries," *Ionics (Kiel)*, vol. 23, no. 2, pp. 377–384, Feb. 2017, doi: 10.1007/s11581-016-1910-z.

[13] S. Wu *et al.*, "Fe2O3/carbon derived from peanut shell hybrid as an advanced anode for high performance lithium ion batteries," *J Energy Storage*, vol. 68, Sep. 2023, doi: 10.1016/j.est.2023.107731.

[14] W. C. Chien, K. N. Liu, S. C. Chang, and C. C. Yang, "Effects of α-Fe2O3 size and morphology on performance of LiFePO4/C cathodes for Li-ion batteries," *Thin Solid Films*, vol. 660, pp. 931–937, Aug. 2018, doi: 10.1016/j.tsf.2018.02.017.

[15] H. M. Cheng, F. M. Wang, and J. P. Chu, "Effect of Lorentz force on the electrochemical performance of lithium-ion batteries," *Electrochem commun*, vol. 76, pp. 63–66, Mar. 2017, doi: 10.1016/j.elecom.2017.01.022.

[16] Q. fang Zhao *et al.*, "Surface modification of LiFePO4 by Coatings for Improving of Lithium-ion Battery Properties," *Int J Electrochem Sci*, vol. 17, 2022, doi: 10.20964/2022.11.31.

[17] C. M. Costa, K. J. Merazzo, R. Gonç, C. Amos, and S. Lanceros-Mé Ndez, "iScience Magnetically active lithium-ion batteries towards battery performance improvement", doi: 10.1016/j.isci.

[18] M. V. Reddy, A. Mauger, C. M. Julien, A. Paolella, and K. Zaghib, "Brief history of early lithium-battery development," *Materials*, vol. 13, no. 8, Apr. 2020, doi: 10.3390/MA13081884.

[19] A. M. Theodore, "Progress into lithium-ion battery research," *J Chem Res*, vol. 47, no. 3, May 2023, doi: 10.1177/17475198231183349.

[20] N. Nakamura, S. Ahn, T. Momma, and T. Osaka, "Future potential for lithium-sulfur batteries," *J Power Sources*, vol. 558, Feb. 2023, doi: 10.1016/j.jpowsour.2022.232566.

[21] M. Xiao and Z. Xing, "Recent Progress of Lithium-Sulfur Batteries," *Batteries*, vol. 9, no. 2. MDPI, Feb. 01, 2023. doi: 10.3390/batteries9020079.

[22] J. Zhang, C. You, H. Lin, and J. Wang, "Electrochemical Kinetic Modulators in Lithium–Sulfur Batteries: From Defect-Rich Catalysts to Single Atomic Catalysts," *Energy and Environmental Materials*, vol. 5, no. 3. John Wiley and Sons Inc, pp. 731–750, Jul. 01, 2022. doi: 10.1002/eem2.12250.

[23] A. Niu, J. Mu, J. Zhou, X. Tang, and S. Zhuo, "Cation Vacancies in Feroxyhyte Nanosheets toward Fast Kinetics in Lithium–Sulfur Batteries," *Nanomaterials*, vol. 13, no. 5, Mar. 2023, doi: 10.3390/nano13050909.

[24] X. Zhang, H. Yang, Y. Sun, and Y. Yang, “Lithium Sulfide: Magnesothermal Synthesis and Battery Applications,” *ACS Appl Mater Interfaces*, vol. 14, no. 36, pp. 41003–41012, Sep. 2022, doi: 10.1021/acsami.2c11196.

[25] R. Cheng *et al.*, “Carbon Coated Metal-Based Composite Electrode Materials for Lithium Sulfur Batteries: A Review,” *Chemical Record*, vol. 22, no. 10. John Wiley and Sons Inc, Oct. 01, 2022. doi: 10.1002/tcr.202200168.

[26] H. Wu, X. Hu, M. Shao, S. Zhang, and G. Chen, “Encapsulating sulphur inside Magnéli phase Ti4O7 nanotube array for high performance lithium sulphur battery cathode,” *Canadian Journal of Chemical Engineering*, vol. 100, no. 9, pp. 2417–2431, Sep. 2022, doi: 10.1002/cjce.24413.

[27] Z. Lin and C. Liang, “Lithium-sulfur batteries: From liquid to solid cells,” *Journal of Materials Chemistry A*, vol. 3, no. 3. Royal Society of Chemistry, pp. 936–958, 2015. doi: 10.1039/c4ta04727c.

[28] Y. Huang *et al.*, “Solvation Structure with Enhanced Anionic Coordination for Stable Anodes in Lithium-Oxygen Batteries,” *Angewandte Chemie - International Edition*, vol. 62, no. 30, Jul. 2023, doi: 10.1002/anie.202306236.

[29] M. Park *et al.*, “Heterogeneous Catalyst as a Functional Substrate Governing the Shape of Electrochemical Precipitates in Oxygen-Fueled Rechargeable Batteries,” *J Am Chem Soc*, vol. 145, no. 28, pp. 15425–15434, Jul. 2023, doi: 10.1021/jacs.3c03619.

[30] N. Feng, C. Wang, J. Wang, Y. Lin, and G. Yang, “A High-Performance Li-O2/Air Battery System with Dual Redox Mediators in the Hydrophobic Ionic Liquid-Based Gel Polymer Electrolyte,” *Batteries*, vol. 9, no. 5, May 2023, doi: 10.3390/batteries9050243.

[31] W. Zhang *et al.*, “Water-Trapping Single-Atom Co-N4/Graphene Triggering Direct 4e− LiOH Chemistry for Rechargeable Aprotic Li–O2 Batteries,” *Small*, vol. 19, no. 33, Aug. 2023, doi: 10.1002/smll.202301391.

[32] C. Dang *et al.*, “NiCoP based carbon nanotube heterostructure for improved oxygen redox reaction kinetics in Li-O2 batteries,” *Electrochim Acta*, vol. 462, Sep. 2023, doi: 10.1016/j.electacta.2023.142771.

[33] J. Zhang *et al.*, “A long-life lithium-oxygen battery via a molecular quenching/mediating mechanism”, doi: 10.21203/rs.3.rs-534571/v1.

[34] C. Wang *et al.*, “Enzyme-Inspired Room-Temperature Lithium–Oxygen Chemistry via Reversible Cleavage and Formation of Dioxygen Bonds,” *Angewandte Chemie - International Edition*, vol. 59, no. 41, pp. 17856–17863, Oct. 2020, doi: 10.1002/anie.202009792.

[35] S. Pakseresht, M. Celik, A. Guler, A. W. M. Al-Ogaili, and T. Kallio, “Recent Advances in All-Solid-State Lithium–Oxygen Batteries: Challenges, Strategies, Future,” *Batteries*, vol. 9, no. 7. Multidisciplinary Digital Publishing Institute (MDPI), Jul. 01, 2023. doi: 10.3390/batteries9070380.

[36] S. Leuthner, “Lithium-ion battery overview,” in *Lithium-Ion Batteries: Basics and Applications*, Springer Berlin Heidelberg, 2018, pp. 13–19. doi: 10.1007/978-3-662-53071-9_2.

[37] J. Zhang, L. Zhang, F. Sun, and Z. Wang, “An Overview on Thermal Safety Issues of Lithium-ion Batteries for Electric Vehicle Application,” *IEEE Access*, vol. 6, pp. 23848–23863, May 2018, doi: 10.1109/ACCESS.2018.2824838.

[38] F. A. Silva, “Lithium-Ion Batteries: Fundamentals and Applications [Book News],” *IEEE Industrial Electronics Magazine*, vol. 10, no. 1, pp. 58–59, Mar. 2016, doi: 10.1109/mie.2016.2515040.

[39] I. H. Sardar and S. Bhattacharyya, “A Short Review of Lithium-ion Battery Technology,” *Int J Sci Res Sci Eng Technol*, pp. 500–507, Apr. 2020, doi: 10.32628/ijsrset207295.

[40] M. Armand *et al.*, “Lithium-ion batteries – Current state of the art and anticipated developments,” *J Power Sources*, vol. 479, Dec. 2020, doi: 10.1016/j.jpowsour.2020.228708.

[41] M. Qin, Z. Zeng, S. Cheng, and J. Xie, “Challenges and strategies of formulating low‐temperature electrolytes in lithium‐ion batteries,” *Interdisciplinary Materials*, vol. 2, no. 2, pp. 308–336, Mar. 2023, doi: 10.1002/idm2.12077.

[42] H. Luo, Y. Wang, Y. H. Feng, X. Y. Fan, X. Han, and P. F. Wang, “Lithium-Ion Batteries under Low-Temperature Environment: Challenges and Prospects,” *Materials*, vol. 15, no. 22. MDPI, Nov. 01, 2022. doi: 10.3390/ma15228166.

[43] X. Yu *et al.*, “Current Challenges in Efficient Lithium-Ion Batteries’ Recycling: A Perspective,” *Global Challenges*, vol. 6, no. 12, Dec. 2022, doi: 10.1002/gch2.202200099.

[44] A. Masias, J. Marcicki, and W. A. Paxton, “Opportunities and Challenges of Lithium Ion Batteries in Automotive Applications,” *ACS Energy Letters*, vol. 6, no. 2. American Chemical Society, pp. 621–630, Feb. 12, 2021. doi: 10.1021/acsenergylett.0c02584.

[45] N. Piao *et al.*, “Challenges and development of lithium-ion batteries for low temperature environments,” *eTransportation*, vol. 11, Feb. 2022, doi: 10.1016/j.etran.2021.100145.

[46] J. Zhou, D. Zhang, G. Sun, and C. Chang, “B-axis oriented alignment of LiFePO4 monocrystalline platelets by magnetic orientation for a high-performance lithium-ion battery,” *Solid State Ion*, vol. 338, pp. 96–102, Oct. 2019, doi: 10.1016/j.ssi.2019.05.002.

[47] Z. Shah *et al.*, “Three dimensional third grade nanofluid flow in a rotating system between parallel plates with Brownian motion and thermophoresis effects,” *Results Phys*, vol. 10, pp. 36–45, Sep. 2018, doi: 10.1016/j.rinp.2018.05.020.

[48] Y. Xu, J. Chen, B. Jiang, Y. Liu, and J. Ni, “Experimental investigation of magnetohydrodynamic effect in electrochemical discharge machining,” *Int J Mech Sci*, vol. 142–143, pp. 86–96, Jul. 2018, doi: 10.1016/j.ijmecsci.2018.04.020.

[49] O. Gutfleisch, M. A. Willard, E. Brück, C. H. Chen, S. G. Sankar, and J. P. Liu, "Magnetic materials and devices for the 21st century: Stronger, lighter, and more energy efficient," *Advanced Materials*, vol. 23, no. 7. pp. 821–842, Feb. 15, 2011. doi: 10.1002/adma.201002180.

[50] A. Manthiram, "A reflection on lithium-ion battery cathode chemistry," *Nature Communications*, vol. 11, no. 1. Nature Research, Dec. 01, 2020. doi: 10.1038/s41467-020-15355-0.

[51] J. Werner, C. Neef, C. Koo, S. Zvyagin, A. Ponomaryov, and R. Klingeler, "Antisite disorder in the battery material LiFePO4," *Phys Rev Mater*, vol. 4, no. 11, Nov. 2020, doi: 10.1103/PhysRevMaterials.4.115403.

[52] G. Hinds, J. M. D. Coey, and M. E. G. Lyons, "In¯uence of magnetic forces on electrochemical mass transport." [Online]. Available: www.elsevier.nl/locate/elecom

[53] M. Ameziane, R. Mansell, V. Havu, P. Rinke, and S. van Dijken, "Lithium-Ion Battery Technology for Voltage Control of Perpendicular Magnetization," *Adv Funct Mater*, vol. 32, no. 29, Jul. 2022, doi: 10.1002/adfm.202113118.

[54] Y. Chen, X. Dou, K. Wang, and Y. Han, "Magnetically enhancing diffusion for dendrite-free and long-term stable lithium metal anodes," *Green Energy and Environment*, vol. 7, no. 5, pp. 965–974, Oct. 2022, doi: 10.1016/j.gee.2020.12.014.

[55] S. Kimura *et al.*, "Magnetization and high-frequency EMR measurements on the lithium-ion battery substance LiMn2O4," *Japanese Journal of Applied Physics, Part 1: Regular Papers and Short Notes and Review Papers*, vol. 44, no. 10, pp. 7440–7444, Oct. 2005, doi: 10.1143/JJAP.44.7440.

[56] Y. Li, X. Sun, H. Wang, H. Lu, and C. Liu, "Academic Journal of Science and Technology A Rapid Depolarization Charge and Discharge Technique for Lithium Ion Batteries".

[57] A. Bund, S. Koehler, H. H. Kuehnlein, and W. Plieth, "Magnetic field effects in electrochemical reactions," in *Electrochimica Acta*, Dec. 2003, pp. 147–152. doi: 10.1016/j.electacta.2003.04.009.

[58] Y. D. Yu, Z. L. Song, H. L. Ge, and G. Y. Wei, "Influence of magnetic fields on cobalt electrodeposition," *Surface Engineering*, vol. 30, no. 2, pp. 83–88, 2014, doi: 10.1179/1743294413Y.0000000229.

[59] L. M. A. Monzon and J. M. D. Coey, "Magnetic fields in electrochemistry: The Lorentz force. A mini-review," *Electrochemistry Communications*, vol. 42. Elsevier Inc., pp. 38–41, 2014. doi: 10.1016/j.elecom.2014.02.006.

[60] W. Zhou *et al.*, "Magnetic Enhancement for Hydrogen Evolution Reaction on Ferromagnetic MoS2 Catalyst," *Nano Lett*, vol. 20, no. 4, pp. 2923–2930, Apr. 2020, doi: 10.1021/acs.nanolett.0c00845.

[61] J. Li *et al.*, "Enhanced Photocatalytic Performance through Magnetic Field Boosting Carrier Transport," *ACS Nano*, vol. 12, no. 4, pp. 3351–3359, Apr. 2018, doi: 10.1021/acsnano.7b08770.

[62] J. Lu, Z. Chen, F. Pan, Y. Cui, and K. Amine, "High-Performance Anode Materials for Rechargeable Lithium-Ion Batteries," *Electrochemical Energy Reviews*, vol. 1, no. 1. Springer Science and Business Media B.V., pp. 35–53, Mar. 01, 2018. doi: 10.1007/s41918-018-0001-4.

[63] M. F. Lagadec, R. Zahn, and V. Wood, "Characterization and performance evaluation of lithium-ion battery separators," *Nature Energy*, vol. 4, no. 1. Nature Publishing Group, pp. 16–25, Jan. 01, 2019. doi: 10.1038/s41560-018-0295-9.

[64] Y. Huang, C. fa Xiao, Q. lin Huang, H. liang Liu, J. qiang Hao, and L. Song, "Magnetic field induced orderly arrangement of Fe3O4/GO composite particles for preparation of Fe3O4/GO/PVDF membrane," *J Memb Sci*, vol. 548, pp. 184–193, Feb. 2018, doi: 10.1016/j.memsci.2017.11.027.

[65] M. Kamel *et al.*, "Synthesis, Optical, Magnetic and Thermodynamic Properties of Rocksalt Li 1.3 Nb 0.3 Mn 0.4 O 2 Cathode Material for Li-Ion Batteries," p. 11, 2021, doi: 10.3390/cryst.

[66] S. Wu *et al.*, "Fe2O3/carbon derived from peanut shell hybrid as an advanced anode for high performance lithium ion batteries," *J Energy Storage*, vol. 68, Sep. 2023, doi: 10.1016/j.est.2023.107731.

[67] X. Wang *et al.*, "Epitaxial Growth of Hexahedral Fe 2 O 3 @SnO 2 Nano-Heterostructure for Improved Lithium-Ion Battery." [Online]. Available: https://ssrn.com/abstract=4336721

[68] Z. Yang, J. Zhu, W. Tang, and Y. Ding, "An Fe2O3/Mn2O3 Nanocomposite Derived from a Metal-Organic Framework as an Anode Material for Lithium-ion Batteries," *ChemistrySelect*, vol. 7, no. 42, Nov. 2022, doi: 10.1002/slct.202203107.

[69] L. Dang *et al.*, "Highly stable Fe23@SnO2@HNCS hollow nanospheres with enhanced lithium-ion battery performance," *New Journal of Chemistry*, vol. 47, no. 6, pp. 3017–3025, Jan. 2023, doi: 10.1039/d2nj05799a.

[70] G. Yang *et al.*, "Integrated co-modification of PO43− polyanion doping and Li2TiO3 coating for Ni-rich layered LiNi0.6Co0.2Mn0.2O2 cathode material of Lithium-Ion batteries," *Chemical Engineering Journal*, vol. 421, Oct. 2021, doi: 10.1016/j.cej.2021.129964.

[71] L. Yang *et al.*, "LiFePO4 nanoplates with {010} exposed active planes prepared by hydrothermal method," *Journal of Materials Science: Materials in Electronics*, vol. 27, no. 11, pp. 12258–12263, Nov. 2016, doi: 10.1007/s10854-016-5383-7.

[1]